Genome-wide Wheat 55K SNP-based Mapping of Stripe Rust Resistance Loci in Wheat Cultivar Shaannong 33 and Their Alleles Frequencies in Current Chinese Wheat Cultivars and Breeding Lines

Shuo Huang[1], Shengjie Liu[1], Yibo Zhang[1], Yanzhou Xie[1], Xiaoting Wang[1], Hanxuan Jiao[1], Shushu Wu[1], Qingdong Zeng[2], Qilin Wang[1], Ravi P. Singh[3], Sridhar Bhavani[3], Zhensheng Kang[2], Chengshe Wang[1†], Dejun Han[1†], and Jianhui Wu[1†]

[1] State Key Laboratory of Crop Stress Biology for Arid Areas, College of Agronomy, Northwest A&F University, Yangling, Shaanxi 712100, P. R. China

[2] State Key Laboratory of Crop Stress Biology for Arid Areas, College of Plant Protection, Northwest A&F University, Yangling, Shaanxi 712100, P. R. China

[3] International Maize and Wheat Improvement Center (CIMMYT), El Batan, Texcoco, Estado de Mexico 56237, Mexico

S. Huang and S. Liu contributed equally to this work.

*Corresponding authors: Chengshe Wang E-mail: wangcs2008@126.com; Dejun Han E-mail: handj@nwafu.edu.cn; Jianhui Wu E-mail: wujh@nwafu.edu.cn

---

Abstract

Wheat cultivar Shannong 33 (SN33) has remained highly resistant to stripe rust in the field since its release in 2009. To unravel the genetic architecture of stripe rust resistance, seedlings of 161 recombinant inbred lines (RILs) from the cross Avocet S × SN33 were evaluated with two isolates (PST-Lab.1 and PST-Lab.2) of the stripe rust pathogen (*Puccinia striiformis* f. sp. *tritici*) in the greenhouse, and the RILs were evaluated in naturally and/or artificially inoculated field sites during two cropping seasons. The RILs and parents were genotyped with the wheat 55K single nucleotide polymorphism (SNP) array. Three genomic regions conferring seedling resistance were mapped on chromosomes 1DS, 2AS, and 3DS, and four consistent quantitative trait loci (QTL) for adult-plant resistance (APR) were detected on 1BL, 2AS, 3DL, and 6BS. The 2AS locus conferring all-stage resistance was identified as the resistant gene *Yr17* located on 2NS translocation. The QTL identified on 1BL and 6BS likely correspond to *Yr29* and *Yr78*, respectively. An APR QTL on 3DL explaining 5.8–12.2% of the phenotypic variation is likely to be new. Molecular marker detection assays with the 2NS segment (*Yr17*), *Yr29*, *Yr78*, and *QYrsn.nwafu-3DL* on a panel of 420 current

Chinese wheat cultivars and breeding lines indicated that these genes were present in 11.4%, 7.6%, 14.8%, and 7.4% entries, respectively. The interactions among these genes/QTL were additive suggesting their potential value in enhancing stripe rust resistance breeding materials as observed in the resistant parent. In addition, we also identified two leaf necrosis genes, *Ne1* and *Ne2*, however, the F_1 plants from cross Avocet S × SN33 survived indicating that SN33 probably has another allele of *Ne1* which allows to harvest seeds.

Common wheat (*Triticum aestivum* L.), one of the most important cereal crops, provides more than 20% of total grain production and feeds 36% of the world population (Singh et al. 2016). It is predicted that with climate change, biotic stresses especially fungal diseases will continue to be a major threat to the maintenance of production levels. Among the three rust diseases, stripe rust or yellow rust, caused by *Puccinia striiformis* Westend. f. sp. *tritici* Erikss. (*Pst*), occurs more frequently in areas with cool conditions during the growing season (Carvajal-Yepes et al. 2019). China was considered one of the largest stripe rust epidemic regions in the world (Stubbs 1985), and frequent epidemics have been reported (Han and Kang 2018). Fungicides can provide effective control when used at the right time. However, when a crop is overwhelmed by high disease pressure and application is too late, fungicide is often ineffective in providing adequate control (Chen 2014). Moreover, chemical control adds to production costs and might have effects on human health and the environment. Therefore, the use of genetic resistance is the preferred strategy to control stripe rust.

Resistance to stripe rust is broadly classified into two groups/categories based on expression at different growth stages; namely, seedling or all-stage resistance (ASR) and adult-plant resistance (APR) or high-temperature adult-plant (HTAP) resistance (Chen 2013). To date, 83 formally named genes for resistance to stripe rust have been catalogued (Li et al. 2020; McIntosh et al. 2017). However, most of the designated stripe rust genes confer ASR that is race-specific and prone to be overcome by the emergence of virulent races following widespread deployment (McIntosh et al. 2018; Niks et al. 2015). There are well documented cases of sequential losses in effectiveness of genes *Yr1*, *Yr3*, *Yr6*, *Yr4*, *Yr9*, and *Yr24* (=*Yr26*) in China (Han and Kang 2018). Race CYR34 is not only virulent to *Yr24* that is deployed in many cultivars in the rust-prone regions of Sichuan, Shaanxi, and Gansu provinces but is also virulent for a number of other previously effective genes including *Yr10*, *Yr17*, *Yr27*, *Yr31*, *Yr41*, *Yr43*, *Yr44*, *Yr50*, and *Yr67* (Huang et al. 2019; Mu et al. 2019b; Wu et al. 2016, 2018a, 2020). Although *Yr5*, *Yr15*, *Yr53*, *Yr61*, *Yr64*, *Yr65*, *Yr69*, and *Yr83* are still effective against CYR34 and other *Yr24*-virulent races, most of them are not available in well-

adapted Chinese germplasm (Han and Kang 2018).

Adult-plant resistance or HTAP resistance is often non-race-specific and determined by combinations of two or more genes or quantitative trait loci (QTL) acting additively and therefore showing quantitative inheritance (Johnson 1984; Niks et al. 2015). Wheat cultivars with only APR are generally susceptible at the seedling stage, but gradually become resistant as plants grow and temperature increases (Chen and Line 1995). Since genetic analyses have consistently shown that diverse sources of highly effective durable resistance are based on combinations of partially effective genes that have additive effects, it is reasonable that a strategy of breeding that ensures gene combinations should be employed for obtaining prolonged resistance (Nelson et al. 2017). Moreover, many of the QTL so far described have been discovered in adapted genetic material and their utilization is less likely to be confronted by linkage drag.

In our previous studies with approximately 2,000 common wheat accessions, including Chinese local landraces, core collections, modern cultivars, and foreign germplasms were screened for stripe rust response under controlled greenhouse conditions and in naturally and artificially inoculated fields since 2008. A large number of accessions with excellent resistance to prevalent Chinese *Pst* races were identified (Han et al. 2015; Mu et al. 2019b). Among them, 'Shaannong 33' (SN33) has exhibited a high level of resistance since its release in 2009 (Mu et al. 2019b; Wu et al. 2016). SN33 was developed from the cross 'Zhoumai 18' × 'Shaanmai 981', and it has been grown on over 80,000 ha in the Yellow and Huai River Valleys. Despite the significant impact of SN33 on increasing wheat production, little is known about the genetic basis of resistance.

To dissect the genetic architecture of *Pst* resistance in SN33, a recombinant inbred lines (RIL) population was developed from cross Avocet S × SN33 and a panel of 420 current Chinese wheat cultivars and breeding lines were evaluated for stripe rust resistance in different environments. The specific objectives of our study were to: 1) map and identify QTL conferring stripe rust resistance in SN33, 2) develop polymerase chain reaction (PCR) markers linked to the corresponding gene/QTL for marker-assisted selection, and 3) evaluate the interaction among these genes/QTL and their frequencies in current Chinese wheat cultivars and breeding lines.

Materials and methods

Plant materials. The F_5-derived F_6 RIL population of 161 lines was developed from cross Avocet S (AvS) × Shaannong 33 (SN33). The Chinese landrace Mingxian 169 (MX169) and cultivar Xiaoyan 22 (XY22) were both used as susceptible controls. VPM 1 (*Yr17*), Hugenoot (*Yr25*), Pavon 76 (*Yr29*), Stephens (*Yr78*), and Madsen (*Yr17+Yr78*)

were also included for comparative analysis. A panel of 420 current Chinese wheat cultivars and breeding lines from winter wheat growing regions were evaluated for resistance to stripe rust across multiple field environments and used to determine the prevalence of resistance genes identified in SN33 based on flanking SNP markers. Furthermore, a set of *Yr* near-isogenic lines in the AvS background, set of Chinese differential cultivars, and certain *Yr* gene donor lines (Table S1) were included in the study as reference stocks for individual *Yr* genes.

Greenhouse trials. Phenotyping for seedling reactions to different *Pst* races was conducted under controlled greenhouse conditions at Yangling, Shaanxi province. Three single spore-derived *Pst* isolates, PST-Lab.1, PST-Lab.2, and PST-V26.1, from predominant *Pst* race groups were used in the study; their avirulence/virulence attributes are described in Table S1. PST-Lab.1 and PST-Lab.2 were developed from two different collections of the predominant *Pst* race CYR32. Five to six seeds of SN33, AvS, and RILs were planted in plastic pots as three sets, and each set of the 14-day old seedlings was inoculated with a single *Pst* isolate. Inoculated plants were incubated at 10°C in a dew chamber in darkness for 24 h, and then transferred to a greenhouse at 17 ± 2 °C with 14 h of light (20,000 lx) daily. Infection types (IT) based on a 0–9 scale (Line and Qayoum 1992) were recorded 18-21 days after inoculation. Lines with IT scores of 0-3 were repeated thrice with the same isolate to validate resistance response.

Field experiments and hybrid necrosis. SN33, AvS, and the 161 RILs were evaluated for stripe rust response at Jiangyou (JY) in Sichuan and Yangling (YL) in Shaanxi provinces in 2017-2018 and 2018-2019, and Tianshui (TS) in Gansu province in 2018-2019. The locations in Sichuan and southern Gansu are cool and wet during late spring and early summer considered ideal sites for stripe rust development. The fields at Yangling were inoculated with *Pst* isolate PST-V26.1 suspended in a light oil (1:300) sprayed onto MX169 and XY22 at flag leaf emergence. Each plot consisted of a 1 m row sown with approximately 30 seeds and 30 cm row spacing. Two rows of spreader XY22 were planted after every 20 rows to ensure uniform disease development. A randomized complete block design with two replicates was used in all experiments. IT and disease severity (DS) were used to evaluate for adult plant reactions. IT was recorded using a 0 (resistant) to 9 (susceptible) scale (Line and Qayoum 1992); DS was scored based on the modified Cobb Scale (Peterson et al. 1948). The first scoring was done when AvS and MX169 reached approximately 80% severity or higher during the period 5–25 April at JY, 3–17 May at YL, and 10–15 June at TS. IT and DS of homozygous lines were recorded as single values; and for segregating lines IT and DS were recorded as two or more values, but later averaged for each line. Disease assessment was made at least twice and, finally, the highest ITs and the

maximum DS (MDS) were used for phenotypic and QTL analyses.

Although leaf necrosis was present at all sites, phenotyping was carried out only at YL. When the flag leaves emerged completely, we evaluated the progress of necrosis as 0 or 1, where 0 = no necrosis in any leaf (Green), 1 = show necrosis in leaves (Yellow), and the segregating lines were scored using the mean values. Necrosis eventually affected the flag leaves making us unable to score stripe rust reactions accurately on necrotic plants. Thus, the lines homozygous for necrosis (serious necrosis) should be deleted in rust analyses (Prof. Robert McIntosh, personal communication).

Phenotypic analysis. Analysis of variance (ANOVA) was conducted using the mean IT and DS data for RILs across five environments to determine the effects of genotype (G), environment (E), and G × E interaction. Pearson's correlation coefficient (r) analysis and ANOVA were conducted using the "AOV" function in QTL IciMapping software 4.1 with the default parameters (Meng et al. 2015). Estimation of broad-sense heritability (*h2 b*) of resistance was based on the equation $h2\ b = \sigma 2\ g/(\sigma 2\ g + \sigma 2\ ge/e + \sigma 2\ \varepsilon/re)$, where $\sigma 2\ g$, $\sigma 2\ ge$, and $\sigma 2\ r$ represent genotypic (RILs), G × E, and error variances, respectively, and *e* and *r* were the numbers of environments and replicates. Based on the phenotypic data including IT and DS across ten environments, the BLUP (best linear unbiased prediction) data were used to evaluate the genetic effects and find a more possible position for QTL detection (Bates et al. 2015).

SNP calling and clustering. DNA of the parents and RILs was extracted from 10-15 plants per line at the jointing stage using the cetyltrimethylammonium bromide (CTAB) protocol (Clarke et al. 2002), and DNA quality and quantity were assessed using a NanoDrop ND-1000 (Thermo Scientific, Wilmington, DE, USA). The wheat 55K SNP array from CapitalBio Corporation (Beijing; http://www.capitalbio.com) was used for genotyping. SNP genotype calling and allele clustering was processed with the polyploid version of the Affymetrix Genotyping Console™ (GTC) software. The SNPs were classified into six groups: (i) PolyHighResolution (PHR) SNPs that were polymorphic and co-dominant with a minimum of two samples containing the minor allele; (ii) No Minor Homozygote (NMH); these polymorphic and dominant SNPs had only two clusters, one being the heterozygote; (iii) Mono High Resolution (MHR) or monomorphic SNPs having only one cluster/allele; (iv) Of-Target Variants (OTV) showing four clusters including one for a null allele; (v) Call Rate Below Threshold (CRBT) having all cluster properties above the threshold except for the call rate cut-of; and (vi) other type SNPs with one or more cluster properties below quality thresholds.

Linkage map construction and QTL analysis. The filtering criteria of SNP markers for linkage map construction were as follows: PolyHighResolution (PHR)/polymorphic, <10% missing values, major allele frequencies (MAF) ≤95%, and

1:1 segregation ratio confirmed by χ^2 tests (P >0.001). A linkage map was constructed using QTL IciMapping V4.1 software and generated with Mapchart V2.3 (Meng et al. 2015; Voorrips 2002). Recombination fractions were converted to centiMorgans (cM) using the Kosambi function (Kosambi 1943). The phenotypic data including IT, DS, and BLUP values were used to identify the QTL. One marker was selected from each co-segregating marker group using the "BIN" function. The selected markers were used to construct the genetic map using the "MAP" function, and inclusive composite interval mapping with the additive tool (ICIM-ADD) and in IciMapping V4.1 was performed to detect QTL for IT and DS. Combining the calculated value by 1000 permutations at a probability of 0.01, the LOD score to determine significant QTL was 4.8 in all five environments. The phenotypic variances explained (PVE) by individual QTL and additive effects at the LOD peaks were also obtained. In addition, inclusive composite interval mapping of digenic epistatic QTL (ICIM-EPI) functionality was also used to detect epistatic interactions between the detected QTL.

Comparisons with previously published *Yr* genes and QTL. To determine the relationships between loci identified in SN33 and previously reported *Yr* genes/QTL, we compared the relative genetic distances of loci based on the integrative genetic maps (Maccaferri et al. 2015; Dr. Fa Cui, personal communication). For previously reported *Yr* genes/QTL, the closest flanking markers were used to generate confidence intervals (Bulli et al. 2016; Chen and Kang 2017; Maccaferri et al. 2015). Whether loci identified in SN33 were new depended on actual stripe rust responses, molecular detection, and relative genetic distances.

The frequencies of identified gene/QTL revealed by linked PCR marker. Based on the mapping results, polymorphic SNP markers flanking the consistent QTL were converted into kompetitive allele specific PCR (KASP) primers and were first used to test the parents and the selected RILs following Wu et al. (2018b). KASP end-point fluorescent images were visualized using a microplate reader (FLUOstar Omega, BMG LABTECH, Offenburg, Germany) and allelic discrimination was determined using Klustering Caller software (LGC, Middlesex, UK). To determine the frequencies of the identified genes/QTL in the Chinese wheat cultivars and breeding lines, KASP-SNP or PCR markers *VENTRIUP/LN2*, *csLV46G22*, and *IWA7257* specific for *Aegilops ventricosa* 2NS (harboring *Yr17*) (Helguera et al. 2003), *Lr46/Yr29* (Ren et al. 2017), and *Yr78* (Dong et al. 2017), respectively, were also used for molecular detection in SN33 (control) and a panel of 420 current Chinese cultivars and breeding lines. In addition, these lines were also phenotyped for stripe rust severity during the 2018-2019 crop season in JY, YL, and TS, and the data were used for the evaluation of the effect of gene combinations.

Results

Phenotypic evaluation. SN33 seedlings displayed resistance (IT 1–2) to PST-Lab.1 and PST-Lab.2 but were susceptible (IT 8–9) to *Pst* isolate PST-V26.1. At the adult-plant stage, SN33 was highly resistant (IT 1–2, DS ≤5%) to all tested isolates (Fig. S1A). AvS was highly susceptible (IT 9) to all races at both growth stages (Fig. S1B). Based on these results, we concluded that SN33 possesses both seedling resistance and APR. In seedling tests with PST-Lab.1 and PST-Lab.2, the RILs showed continuous IT distribution and could not be clearly classified into resistant and susceptible classes (Fig. 1A and B). Thus, seedling resistance to PST-Lab.1 and PST-Lab.2 was quantitatively inherited.

In field experiments, AvS was susceptible (IT 8-9, DS ≥80) and SN33 was resistant (IT 0–3, DS ≤10). Both IT and MDS data for RILs showed continuous and normal distributions (Fig. 1C, D, E, and F), indicating that APR in SN33 was quantitatively inherited. Pearson's correlation coefficients of pairwise comparison for IT and DS ranged from 0.62-0.81 and 0.61-0.83 (P <0.001) (Table 1), respectively. Both IT and DS data for the broad-sense heritability values were 0.90 (Table 2). P values in the ANOVA for IT and DS values showed significant differences (P <0.0001) among RILs, environments, and line × environment interactions. However, the lack of significant variation between the replicates suggested that the resistance genes in RIL population were the main source of phenotypic variation (Table 2). The resistance of SN33 at the adult-plant stage in the field in comparison with the susceptibility of AvS are illustrated in Fig. S1A and B. These results indicated that the expression of QTL controlling APR was consistent across all five environments.

Genetic linkage map. Among 53,063 SNPs, 12,294 (23.17%) showed PHR/polymorphism in the entire RIL population. Among these polymorphic SNPs, 401 were removed due to >10% missing data or distorted segregation. The remaining 11,893 SNPs fell into 2,577 bins. After removing 9,316 redundant SNPs, 2,577 were chosen to represent the corresponding bins and were used to construct the genetic linkage map; they were distributed in 31 linkage groups spanning a total length 4,772.88 cM. The A, B, and D genomes included 925 (39.98%), 1,067 (39.49%), and 585 (20.52%) markers covering lengths of 1,604.16, 1,617.91, and 1,550.81 cM with average marker intervals of 2.96, 2.90, and 1.57 cM, respectively. Chromosomes 1A, 1B, 1D, 2A, 2D, 3A, 3B, 4A, 4D, 6A, 6B, 7A, 7B, and 7D each had a single linkage group; the other chromosomes had two or more groups (Table S2).

QTL mapping for seedling resistance. QTL on chromosomes 1DS (*QYrsn.nwafu-1DS*), 2AS (*QYrsn.nwafu-2AS.1*), and 3DS (*QYrsn.nwafu-3DS*) were identified using seedling test data (Table 3; Fig. S2). The consistent QTL *QYrsn.nwafu-1DS* flanked by

markers *AX-110480216* and *AX-111475929*, explained 6.5 and 31.5% of the phenotypic variation in data obtained using PST-Lab.1 and PST-Lab.2, respectively. *QYrsn.nwafu-2AS.1* flanked by markers *AX-108853005* and *AX-109973606* explained 16.0% of the variation in the seedling test with isolate PST-Lab.1. *QYrsn.nwafu-3DS* with smaller effect, flanking the markers *AX-109446046* and *AX-94498685*, explained 9.4% of the phenotypic variation (Table 3). The QTL *QYrsn.nwafu-1DS* had different resistance response; resistance was higher against PST-Lab.2 but significantly lower against PST-Lab.1. *QYrsn.nwafu-2AS.1* and *QYrsn.nwafu-3DS* gave higher (16.0%) and lower (9.4%) effects, respectively, and were only detected in seedling tests with PST-Lab.1. When tested with PST-V26.1, SN33, AvS, VPM 1, and Madsen were all susceptible.

QTL analysis for APR to stripe rust and QTL combinations in RILs. Both IT and DS data from five field environments were used to detect QTL. Four consistent QTL on chromosome arms 1BL, 2AS, 3DS, and 6BS, designated *QYrsn.nwafu-1BL*, *QYrsn.nwafu-2AS.2*, *QYrsn.nwafu-3DL*, and *QYrsn.nwafu-6BS*, respectively, were identified in all environments and using the BLUP. All detected QTL were derived from the resistant parent SN33 (Table 3; Fig. 2). Among these QTL, *QYrsn.nwafu-1BL*, closely linked to markers *AX-86184925* and *AX-111713183*, explained 4.2-18.9% and 5.0-18.6% of IT and DS variations, respectively (Fig. 2A). *QYrsn.nwafu-2AS.2* located in a 2 cM interval spanned by *AX-109357922* and *AX-109973606*, explained 10.4–36.1% and 13.5–33.0% of the phenotypic variation across environments in IT and DS, respectively (Fig. 2C). *QYrsn.nwafu-3DL* flanked by *AX-94499713* and *AX-108814752* and explained 5.8-12.2% and 8.4-12.2% in the tests with IT and DS data (Fig. 2E). *QYrsn.nwafu-6BS*, linked to *AX-110602591* and *AX-110199811*, explained 6.5–18.5% (IT) and 7.1–15.1% (DS) of the phenotypic variance. Most confidence intervals for this QTL overlapped a 7.0 cM region flanked by the markers *AX-110086144* and *AX-108908139* (Fig. 2G). All these QTL had additive effects for APR to stripe rust.

Different QTL combination had different stripe rust severity reduction. To determine the effects of individual QTL and QTL combinations, RILs were classified into six genotypic groups based on the field tests in YL, JY, and TS (Fig. 3, Table S3). In the field tests, RILs with four QTL *QYrsn.nwafu-1BL*, *QYrsn.nwafu-2AS.2*, *QYrsn.nwafu-3BS*, and *QYrsn.nwafu-3DL* were more resistant (lower IT and DS) than all of the others, displaying almost similar resistance levels to SN33 (Fig. 3). These results indicated that the additive effects of the individual QTL and more QTL in a combination determined higher resistance.

Additive effects were detected for all QTL in both seedling adult-plant tests (Table 3). In seedling tests, three QTL with low additive effects (-0.6 to -1.6), probably due to their race specificity. According to the field tests, the additive effects of IT were in a

range from -0.4 to -1.3, and those of DS ranged from -5.6 to -14.9. Based on the seedling and field tests, the disease reduction by additive effects of individual QTL was influenced by the phenotype data (IT and DS) and different environments.

Mapping of genes contributing to leaf necrosis. The leaf necrosis, or hybrid necrosis, controlled by the interaction of complementary dominant genes *Ne1* (on chromosome arm 5BL) and *Ne2* (on chromosome arm 2BS) (Zhang et al. 2016), was observed in the field experiments. As expected, the parents did not show necrosis, but 27 RILs showed the phenotype, of which 12 RILs were excluded from the mapping analysis for stripe rust QTL because of yellowing on flag leaves in YL (Fig. S1C). Two QTL on 2BS and 5BL were detected in the RIL population, and shown to be *Ne2* (*QNesn.nwafu-2BS*) contributed by AvS with the closet markers *110672470* and *AX-111559203* and *Ne1* (*QNesn.nwafu-5BL*) by SN33 flanked by the markers *AX-109338502* and *AX-108885332*.

Comparisons with previously known *Yr* genes. Three PCR markers linked to previously reported loci *Yr17*, *Yr29*, and *Yr78* were assayed on AvS, SN33, and wheat lines with those genes (Table S4). All except *csLV46G22* were detected in SN33. New KASP markers linked to *QYrsn.nwafu-1BL*, *QYrsn.nwafu-3DL*, and *QYrsn.nwafu-6BS* were also assayed on wheat lines Pavon 76 (*Yr29*, chr. 1BL), VPM 1 (*Yr17*, chr. 2AS), PI 181434 (*Yr45*, chr. 3DL), Stephens (*Yr78*, chr. 6BS), and Madsen (*Yr17*+*Yr78*) (Fig. S3). These results showed that SN33 shared the alleles of *Yr17* with VPM 1 and *Yr78* with Stephens and Madsen, indicating that SN33 likely carry these genes.

Comparative analyses of genetic positions and stripe rust responses were also carried out based on the integrative genetic map. *Yr24* (=*Yr26*) and *Yr29* were previously mapped on chr. 1BL. *QYrsn.nwafu-1BL* conferring partial APR in the field was located within the region 212.7 to 217.8 cM in the genetic map and corresponding to 661.9 to 668.7 Mb in the physical map overlapped the region of the *Yr29* locus. In molecular detection assay, however, AvS and SN33 did not produce the positive band of *csLV46G22*. Further studies are needed to determine the relationship of *QYrsn.nwafu-1BL* with *Yr29*.

QYrsn.nwafu-2AS.1, *QYrsn.nwafu-2AS.2*, and *Yr17* clustered to the terminal region of chromosome 2AS. *Yr17* originated from the 2NS chromosome of *Aegilops ventricosa* (syn. *Triticum ventricosum*) introgressed to the hexaploid wheat lines VPM1 and then to Madsen. SN33 with *QYrsn.nwafu-2AS.1* and AvSYr17NIL conferred seedling resistance (IT 1-2) to PST-Lab.1 but had intermediate to high ITs (3-7) to PST-Lab.2 and PST-V26.1. In addition, these lines also harboring *QYrsn.nwafu-2AS.2* conferred APR in all field tests. AvSYr17NIL, VPM1, Madsen, and SN33 were susceptible at seedling stage but displayed partial APR in fields (Mu et al. 2019b; Wu

et al. 2016). These results suggested that *QYrsn.nwafu-2AS.1* should be *Yr17*, and that *QYrsn.nwafu-2AS.2* was also corresponding to *Yr17* as they all located in the same region.

QYrsn.nwafu-6BS was mapped to a resistance gene-rich region (Dong et al. 2017) harboring *Yr36*, *Yr78*, and other QTL. Previous studies have confirmed that several APR QTL such as *QYr.wgp-6B.1* in Stephens, *QYr.sun-6BS* in Janz, and *QYrMa.wgp-6BS* in Madsen are synonymous of *Yr78* (Liu et al. 2018). Likewise, our results showed the presence the "T" allele for the closest marker, *IWA7257*, in SN33, Stephens, and Madsen, and the "G" allele in AvS indicating that *QYrsn.nwafu-6BS* is likely *Yr78*. The linked markers *IWA7257* for *Yr78* and *AX-109408478* for *QYrsn.nwafu-6BS* were located at 98,033,320 and 118,028,360 bp, respectively.

Frequencies of *Yr17*, *Yr29*, *Yr78*, and *QYrsn.nwafu-3DL* in Chinese wheat germplasm. PCR marker *VENTRIUP/LN2* representing the 2NS segment harboring *QYrsn.nwafu-2AS* (*Yr17*), KASP markers or combinations *AX-86184925*, *AX-109408478* + *IWA7257*, and *AX-109466386* representing *QYrsn.nwafu-1BL* (*Yr29*), *QYrsn.nwafu-6BS* (*Yr78*), and *QYrsn.nwafu-3DL*, respectively, were used to genotype the panel of 420 current Chinese cultivars and breeding lines (Table S4, Table S5). The frequencies of *Yr17*, *Yr29*, *Yr78*, and *QYrsn.nwafu-3DL* based on markers were 11.4% (48 lines), 7.6% (32), 14.8% (62), and 7.4% (31), respectively.

Discussion

Race CYR34 of *Pst*, represented by isolate PST-V26.1 in this study, is virulent to a number of *Yr* genes in addition to *Yr24* and therefore narrowed down the options such as *Yr10* and *Yr24/26/CH42/Gn22* available to wheat breeders. Expanding the numbers of effective resistance genes is an ongoing task. In a previous study, SN33 was identified to display APR to stripe rust in field environments since its release in 2009 (Han et al. 2012). The present study showed that the high level and potentially durable resistance in SN33 was controlled by a combination of known race-specific and APR genes with additive effects. Those genes included *Yr17* and *Yr78*, also ASR QTL on 1DS and 3DS, and APR QTL on 1BL and 3DL.

Yr25 is the only designated gene on 1DS and its more detailed chromosomal location is unknown (Chen and Kang 2017). The reference line Hugenoot for *Yr25* was susceptible in the present study and to PST-V26.1 in a previous study. Eight QTL have been reported on chr. 1D, five from biparental populations including *QYrdr.wgp-1DS* in Druchamp (Hou et al. 2015), *QYr.caas-1DS* in Naxos (Ren et al. 2012), *QYrst.orr-1DS* in Stephens (Vazquez et al. 2012), *QYr.sun-1D* in CPI133872 (Zwart et al. 2010), *YrCEN* in Centrum (Mu et al. 2019a), and three detected in genome-wide association

studies included *QYr.wpg-1D.1* (Naruoka et al. 2015), *QYr.ucw-1D* (Maccaferri et al. 2015), and *QYr.nwafu-1DS.1* (Wu et al. 2020). Among these QTL, *YrCEN*, *QYr.nwafu-1DS.1*, and *QYr.wpg-1D.1* were characterized as ASR genes in common with *QYrsn.nwafu-1DS*. Based on an integrated genetic map and physical position (Bulli et al. 2016), *QYr.nwafu-1DS.1* with flanking markers *AX-110480216* and *AX-111475929*, was located from 9,235,355 bp to 10,404,607 at the distal of chromosome 1DS and only *QYr.wpg-1D.1* with linked marker *IWA6960* at 8,184,770 was in a similar location (Fig. S2B).

QYrsn.nwafu-3DS was identified only in the seedling test with isolates PST-Lab.1 and PST-Lab.2, while *QYrsn.nwafu-3DL* conferred consistent APR in all field environments (Table 2). *QYrsn.nwafu-3DS* was mapped about 50 cM from *QYrsn.nwafu-3DL* on chr. 3DL (Fig. 2E, Fig. S2E). Genes/QTL reported in previous studies included *Yr45* in PI 181434 and PI 660056, *Yr49* in Chuanmai 18, *Yr66* in AGG91584WHEA and AGG91586WHEA, *Yr71* in Sunco (unpublished according to McIntosh et al. 2017), *Yr73* (*YrA*) in Avocet R (Dracatos et al. 2016), *QYr.tam-3D* in Quaiu 3 (Basnet et al. 2014), *QYr-3DS* (Singh et al. 2000) and *QYR6* (Boukhatem et al. 2002) in Optata 85, and *QYr.inra-3D* in Récital (Dedryver et al. 2009). Among these genes on chr. 3DS, only *Yr66* was known as ASR and *QYrsn.nwafu-3DS* overlapped with the region indicated for *Yr66* based on the integrated genetic map, suggesting that *QYrsn.nwafu-3DS* could be *Yr66*. In previous studies, there were three designated gene (*Yr45*, *Yr71*, and *Yr73*) on 3DL. Apparently, *Yr73* (*YrA*), conferring ASR, was different from *QYrsn.nwafu-3DL*. The polymorphic SNP marker *AX-109466386*, linked to *QYrsn.nwafu-3DL*, was used to genotype the parents and the *Yr45* carrier PI 181434. The result showed that SN33 carried a different allele than PI 181434 and AvS. Thus, *QYrsn.nwafu-3DL* should not be *Yr45* (Fig. S3). Comparisons of the physical positions on chromosome 3DL showed that the *Yr71*-linked markers KASP_17207 and KASP_16434 (Bariana et al. 2016) were located at 598,356,516 and 614,366,302 bp, respectively, whereas *QYrsn.nwafu-3DL* linked marker *AX-109582945* was located near 407,401,578 bp. These results indicated that *Yr71* location was far from *QYrsn.nwafu-3DL*. Although *QYrsn.nwafu-3DL* was near to *QYr.tam-3D*, *QYr.inra-3D*, and *QYr.cim-3D* in the integrated genetic map (Fig. 2F), their physical positions based on the Chinese Spring genome are also well separated. *QYrsn.nwafu-3DL* was a consistent QTL with a medium effect (*PVE* = 5.8-12.2%) detected in all five environments (Table 3), whereas *QYr.tam-3D*, *QYr.inra-3D*, and *QYr.cim-3D* were environment dependent QTL detected in one or two environments. Récital harboring *QYr.inra-3D* was susceptible in Chinese field tests (Dejun Han, unpublished data). These results showed that *QYrsn.nwafu-3DL* is likely a new QTL. Flanking marker *AX-109466386* at 180,398,197 bp was polymorphic among 420 Chinese cultivars and thus

can be used for MAS. As a novel resistance QTL, *QYrsn.nwafu-3DL* can contribute to durable resistance through marker-assisted pyramiding with other known APR or ASR genes.

As a major source of resistance, *Yr17* was introduced into northern European wheat cultivars in the mid-1970s. Subsequently, this resistance gene was widely used in breeding programs worldwide and is also present in many cultivars in China. Although *Yr17* was originally considered as a seedling (all-stage) resistance gene and virulent *Pst* isolates detected since 1995 (Bayles et al. 2000), expression of *Yr17* resistance varied with genetic background, pathogen isolate and environmental conditions in later studies. Milus et al. (2015) demonstrated that some factors need to be considered when evaluating *Yr17* reactions at the seedling stage such as night temperatures over 12°C, assessment of the seedling reaction on the first leaves of multiple differentials with *Yr17*, and known avirulent, partially virulent, and virulent isolates as controls, etc. In addition, several researchers found that cultivars with *Yr17* showed intermediate to high ITs to *Yr17*-avirulent isolates in seedling tests despite its effectiveness at adult-plant stages (Bayles and Herron 1987; Fang et al. 2011). *Yr17* conferred intermediate resistance when present alone however displayed adequate resistance when combined with other genes/QTL against prevalent races in tested environments (Coriton et al. 2019; Singh R.P. unpublished results). Liu et al. (2018) hypothesized that the 2NS translocated region contains at least one gene in addition to *Yr17*, and the group has successfully obtained mutant lines with HTAP resistance from the *Yr17* near-isogenic line with *Yr17* demolished (Y. X. Li and X. M. Chen, unpublished data). In the present study, the *Yr17* carriers displayed various responses (IT 1-7) to different races but moderate to high resistance in fields at adult plant stage. These observations were consistent with the hypothesis of HTAP resistance that is affected by temperature, growth stage, and disease pressure.

QYrsn.nwafu-1BL was detected near the distal end of chromosome arm 1BL. Several stripe rust APR QTL in chromosome 1BL have been reported, most of which correspond to the *Yr29/Lr46* locus (Rosewarne et al. 2013; Singh et al. 1998). The result showed that the *Yr29/Lr46* linked marker *csLV46G22* was negative in SN33 and the KASP markers *AX-86184925* linked to *QYrsn.nwafu-1BL* also showed different allele between SN33 and *Yr29* carriers. However, the presence of *Yr29* in SN33 cannot be ruled out as the marker *csLV46G22* is not known to be diagnostic. Also, similar results were found in other mapping populations (Zeng et al. 2019; R. P. Singh unpublished results). Dong et al. (2017) suggested that *QYr.sun-6BS* in Janz, *QYr.wgp-6B.1* in Stephens, and *QYr.wsu-6B.1* could be designated as synonymous of *QYr.ucw-6B* (named as *Yr78*). *QYrsn.nwafu-6BS* was also located in a similar region and shared the

same alleles at the KASP markers loci indicating that *QYrsn.nwafu-6BS* was likely to be *Yr78*. *QYrsn.nwafu-3DL*, conferring APR, was detected as a novel gene. Further studies are required to dissect the chromosomal regions and confirm the genetic relationships among the *Yr* genes/QTL on 1BL, 3DL, and 6BS.

The characteristics of wheat hybrid necrosis are progressive chlorosis and necrosis of plant leaf and sheath tissues, which is controlled by the interaction of complementary dominant genes *Ne1* and *Ne2* on chromosomes 5BL and 2BS, respectively (Chu et al. 2006; Zhang et al. 2016). In Mexico, the hybrid necrosis genes *Ne1* and *Ne2* completely kill F_1 plants in 3-4 weeks resulting in no seed production. In the present study, RILs with weak or medium degree of chlorosis and necrosis were observed among RILs carrying the complementary genes *Ne1* and *Ne2*. *QNesn.nwafu-2BS* and *QNesn.nwafu-5BL*, which were associated with alleles of *Ne2* and *Ne1*, respectively were detected in our RIL population. However, the F_1 plants from the cross AvS × SN33 survived indicating that SN33 probably has another allele of *Ne1* which allows to harvest seeds.

In previous studies, there were 9.11% (45) of 494 cultivars and 10.4% (19) of 183 advanced wheat breeding lines from winter wheat growing regions in China to have the specific marker linked to *Yr17*, respectively (Wu et al. 2016; Zeng et al. 2014). There were 38.5% (37) of 96 wheat breeding lines from Sichuan province to have *Yr29* (Liu et al. 2015). There were 63% of 620 genotyped lines from three recent CIMMYT international spring wheat screening nurseries were positive for the *Yr78* marker (Huerta-Espino et al. 2019). All of the above results indicated that *Yr17*, *Yr29*, and *Yr78* were widely used or common in China since 1980s through germplasm exchange with CIMMYT and other sources. In the present study, it was noted that most of the carriers of *Yr17*, *Yr29*, *Yr78*, and *QYrsn.nwafu-3DL* were from Sichuan, Shaanxi, and Henan where stripe rust occurs very frequently. This observation probably reflects the regular selection for stripe rust resistance by breeders in these provinces although the individual genes alone do not reduce disease severity to acceptable levels under epidemic conditions. Consequently, these genes are selected as important components of unknown gene combinations, and it is only the effectively pyramided lines that are ultimately accepted for release.

Finally, *Yr17*, *Yr29*, *Yr78*, and *QYrsn.nwafu-3DL* are partially effective stripe rust resistance genes that in combination, and preferably in further combination with other partially effective genes, can provide very high levels of potentially durable resistance in hot spot regions of China. Shaannong 33 has a role to play as a breeding parent in achieving that goal.

Funding: This study was financially supported by National Natural Science Foundation of China (Grant no. 31971890), National Science Foundation for Young Scientists in China (Grant no. 31901494 & 31901869), International Cooperation and Exchange of the National Natural Science Foundation of China (Grant no. 31961143019), Opening Foundation of the State Key Laboratory of Crop Biology (2019KF01), China Postdoctoral Science Foundation funding (2019M653769), National "111 plan" (no. BP0719026), and Natural Science Basic Research Plan in Shaanxi Province of China (no. 2019JCW-18).

Literature Cited

Bariana, H., Forrest, K., Qureshi, N., Miah, H., Hayden, M., and Bansal, U. 2016. Adult plant stripe rust resistance gene *Yr71* maps close to *Lr24* in chromosome 3D of common wheat. Mol. Breed. 36:98.

Basnet, B. R., Singh, R. P., Ibrahim, A. M. H., Herrera-Foessel, S. A., Huerta-Espino, J., Lan, C., and Rudd, J. C. 2014. Characterization of *Yr54* and other genes associated with adult plant resistance to yellow rust and leaf rust in common wheat Quaiu 3. Mol. Breed. 33:385-399.

Bates, D., Mächler, M., Bolker, B. M., and Walker, S. C. 2015. Fitting linear mixed-effects models using lme4. J. Stat. Softw. 67:1-48.

Bayles, R. A., and Herron, C. M. 1987. Yellow rust of wheat. Pages 15-20 in: UK Cereal Pathogen Virulence Report for 1986. NIAB, Cambridge, England.

Bayles, R. A., Flath, K., Hovmøller, M. S., and de Vallavielle-Pope, C. 2000. Breakdown of the *Yr17* resistance to yellow rust of wheat in Northern Europe. Agronomy 20:805–811.

Boukhatem, N., Baret, P. V., Mingeot, D., and Jacquemin, J. M. 2002. Quantitative trait loci for resistance against yellow rust in two wheat-derived recombinant inbred line populations. Theor. Appl. Genet. 104:111-118.

Bulli, P., Zhang, J., Chao, S., Chen, X. M., and Pumphrey, M. 2016. Genetic architecture of resistance to stripe rust in a global winter wheat germplasm collection. G3 6:2237-2253.

Carvajal-Yepes, M., Cardwell, K., Nelson, A., Garrett, K. A., Giovani, B., Saunders, D. G. O., Kamoun, S., Legg, J. P., Verdier, V., Lessel, J., Neher, R. A., Day, R., Pardey, P., Gullino, M. L., Records, A. R., Bextine, B., Leach, J. E., Staiger, S., and Tohme, J. 2019. A global surveillance system for crop diseases. Science 364:1237-1239.

Chen, X. M. 2013. High-temperature adult-plant resistance, key for sustainable control of stripe rust. Am. J. Plant Sci. 04:608-627.

Chen, X. M. 2014. Integration of cultivar resistance and fungicide application for control of wheat stripe rust. Can. J. Plant Pathol. 36:311-326.

Chen, X. M., and Kang, Z. S. 2017. Stripe Rust: Springer, the Netherlands.

Chen, X. M., and Line, R. F. 1995. Gene number and heritability of wheat cultivars

518 with durable, high-temperature, adult-plant (HTAP) resistance and interaction of
519 HTAP and race-specific seedling resistance to *Puccinia striiformis*. Phytopathology
520 85:573-578.

521 Chu, C. G., Faris, J. D., Friesen, T. L., and Xu, S. S. 2006. Molecular mapping of hybrid
522 necrosis genes *Ne1* and *Ne2* in hexaploid wheat using microsatellite markers. Theor.
523 Appl. Genet. 112:1374-1381.

524 Clarke, J. D. 2002. Cetyltrimethyl ammonium bromide (CTAB) DNA miniprep for
525 plant DNA isolation. In: Weigel D, Glazebrook J (eds) Arabidopsis: A Laboratory
526 Manual. CSHL Press. Cold Spring Harbor, NY, USA.

527 Coriton, O., Jahier, J., Leconte, M., Huteau, V., Trotoux, G., Dedryver, F., de
528 Vallavieille-Pope, C., and Miedaner, T. 2019. Double dose efficiency of the yellow
529 rust resistance gene *Yr17* in bread wheat lines. Plant Breed. 139:263-271.

530 Dedryver, F., Paillard, S., Mallard, S., Robert, O., Trottet, M., Negre, S., Verplancke,
531 G., and Jahier, J. 2009. Characterization of genetic components involved in durable
532 resistance to stripe rust in the bread wheat 'Renan'. Phytopathology 99:968-973.

533 Dong, Z., Hegarty, J. M., Zhang, J., Zhang, W., Chao, S., Chen, X., Zhou, Y., and
534 Dubcovsky, J. 2017. Validation and characterization of a QTL for adult plant
535 resistance to stripe rust on wheat chromosome arm 6BS (*Yr78*). Theor Appl. Genet.
536 130:2127-2137.

537 Dracatos, P. M., Zhang, P., Park, R. F., McIntosh, R. A., and Wellings, C. R. 2016.
538 Complementary resistance genes in wheat selection 'Avocet R' confer resistance to
539 stripe rust. Theor. Appl. Genet. 129:65-76.

540 Fang, T., Campbell, K. G., Liu, Z., Chen, X., Wan, A., Li, S., Liu, Z., Cao, S., Chen,
541 Y., Bowden, R., Carver, B. F., and Yan, L. 2011. Stripe rust resistance in the wheat
542 cultivar Jagger is due to *Yr17* and a novel resistance gene. Crop Sci. 51:2455-2465.

543 Han, D., and Kang, Z. 2018. Current status and future strategy in breeding wheat for
544 resistance to stripe rust in China. Plant Protection. 44:1-12. [In Chinese with English
545 summary].

546 Han, D., Zhang, P., Wang, Q., Zeng, Q., Wu, J., Zhou, X., Wang, X., Huang, L., and
547 Kang, Z. 2012. Identification and evaluation of resistance to stripe rust in 1980 wheat
548 landraces and abroad germplasm. Sci. Agric. Sin. 45:5013-5023. [In Chinese with
549 English summary].

550 Han, D. J., Wang, Q. L., Chen, X. M., Zeng, Q. D., Wu, J. H., Xue, W. B., Zhan, G.
551 M., Huang, L. L., and Kang, Z. S. 2015. Emerging *Yr26*-virulent races of *Puccinia*
552 *striiformis* f. sp. *tritici* are threatening wheat production in the Sichuan Basin, China.
553 Plant Dis. 99:754-760.

554 Helguera, M., Khan, I. A., Kolmer, J., Lijavetzky, D., Zhong-qi, L., and Dubcovsky, J.
555 2003. PCR assays for the *Lr37-Yr17-Sr38* cluster of rust resistance genes and their
556 use to develop isogenic hard red spring wheat lines. Crop Sci. 43:1839

557 Hou, L., Chen, X., Wang, M., See, D. R., Chao, S., Bulli, P., and Jing, J. 2015 Mapping
558 a large number of QTL for durable resistance to stripe rust in winter wheat Druchamp
559 using SSR and SNP markers. PloS One 10: e0126794.

560 Huang, S., Wu, J., Wang, X., Mu, J., Xu, Z., Zeng, Q., Liu, S., Wang, Q., Kang, Z., and
561 Han, D. 2019. Utilization of the genome-wide wheat 55K SNP array for genetic
562 analysis of stripe rust resistance in common wheat line P9936. Phytopathology

563 109:819-827.

564 Huerta-Espino, J., Crespo-Herrera, L., Dreisigacker, S., Singh, R. P., and Payne, T.
565 2019. Frequency and role of *Yr78* in recent CIMMYT bread wheat. Page 124 in: 1st
566 Int Wheat Congress. C. Pozniak ed. Saskatoon, Saskatchewan, Canada.
567 https://2019iwc.ca/.

568 Johnson, R. 1984. A critical analysis of durable resistance. Annu. Rev. Phytopathol.
569 22:309-330.

570 Kosambi, D. D. 1943. The estimation of map distances from recombination values. Ann.
571 Eugen. 12:172-175.

572 Li, J., Dundas, I., Dong, C., Li, G., Trethowan, R., Yang, Z., Hoxha, S., and Zhang, P.
573 2020. Identification and characterization of a new stripe rust resistance gene *Yr83* on
574 rye chromosome 6R in wheat. Theor. Appl. Genet. 133:1095-1107.

575 Line, R. F., and Qayoum, A. 1992. Virulence, aggressiveness, evolution, and
576 distribution of races of *Puccinia striiformis* (the cause of stripe rust of wheat) in
577 North America 1968-1987. Tech. Bull. No. 1788. USDA-ARS, Washington, DC,
578 U.S.A.

579 Liu, J., Yang, E., Xiao, Y., Chen, X., Wu, L., Bai, B., Li, Z., Garry, M. R., Xia, X., and
580 He, Z. 2015. Development, field and molecular characterization of advanced lines
581 with pleiotropic adult-plant resistance in common wheat. Acta. Agron. Sinica.
582 41:1472-1480.

583 Liu, L., Wang, M. N., Feng, J. Y., See, D. R., Chao, S. M., and Chen, X. M. 2018.
584 Combination of all-stage and high-temperature adult-plant resistance QTL confers
585 high-level, durable resistance to stripe rust in winter wheat cultivar Madsen. Theor.
586 Appl. Genet. 131:1835-1849.

587 Maccaferri, M., Zhang, J., Bulli, P., Abate, Z., Chao, S., Cantu, D., Bossolini, E., Chen,
588 X., Pumphrey, M., and Dubcovsky, J. 2015. A genome-wide association study of
589 resistance to stripe rust (*Puccinia striiformis* f. sp. *tritici*) in a worldwide collection
590 of hexaploid spring wheat (*Triticum aestivum* L.). G3 5:449-465.

591 McIntosh, R., Mu, J., Han, D., and Kang, Z. 2018. Wheat stripe rust resistance gene
592 *Yr24/Yr26*: A retrospective review. Crop J. 6:321-329.

593 McIntosh, R. A., Dubcovsky, J., Rogers, J., Morris, C., Appels, R., and Xia, X. C. 2017.
594 Catalogue of gene symbols for wheat: 2017 Supplement.
595 http://www.shigen.nig.ac.jp/wheat/komugi/genes/macgene/supplement2017.pdf.

596 Meng, L., Li, H. H., Zhang, L. Y., and Wang, J. K. 2015. QTL IciMapping: Integrated
597 software for genetic linkage map construction and quantitative trait locus mapping
598 in biparental populations. Crop J. 3:269-283.

599 Milus, E. A., Lee, K. D., and Brown-Guedira, G. 2015. Characterization of stripe rust
600 resistance in wheat lines with resistance gene *Yr17* and implications for evaluating
601 resistance and virulence. Phytopathology 105:1123-1130

602 Mu, J., Dai, M., Wang, X., Tang, X., Huang, S., Zeng, Q., Wang, Q., Liu, S., Yu, S.,
603 Kang, Z., and Han, D. 2019a. Combining genome-wide linkage mapping with
604 extreme pool genotyping for stripe rust resistance gene identification in bread wheat.
605 Mol. Breed. 39:82.

606 Mu, J., Wang, Q., Wu, J., Zeng, Q., Huang, S., Liu, S., Yu, S., Kang, Z., and Han, D.
607 2019b. Identification of sources of resistance in geographically diverse wheat

accessions to stripe rust pathogen in China. Crop Prot. 122:1-8.

Naruoka, Y., Garland-Campbell, K. A., and Carter, A. H. 2015. Genome-wide association mapping for stripe rust (*Puccinia striiformis* f. sp. *tritici*) in US Pacific Northwest winter wheat (*Triticum aestivum* L.). Theor. Appl. Genet. 128:1083-1101.

Nelson, R., Wiesner-Hanks, T., Wisser, R., and Balint-Kurti, P. 2017. Navigating complexity to breed disease-resistant crops. Nat. Rev. Genet. 19:21-33.

Niks, R. E., Qi, X., and Marcel, T. C. 2015. Quantitative resistance to biotrophic filamentous plant pathogens: concepts, misconceptions, and mechanisms. Annu. Rev. Phytopathol. 53:445-470.

Peterson, R. F., Campbell, A. B., and Hannah, A. E. 1948. A diagrammatic scale for estimating rust intensity on leaves and stems of cereals. Can. J. Res. 26:496-500.

Ren, Y., He, Z., Li, J., Lillemo, M., Wu, L., Bai, B., Lu, Q., Zhu, H., Zhou, G., Du, J., Lu, Q., and Xia, X. 2012. QTL mapping of adult-plant resistance to stripe rust in a population derived from common wheat cultivars Naxos and Shanghai 3/Catbird. Theor. Appl. Genet. 125:1211-1221.

Ren, Y., Singh, R. P., Basnet, B. R., Lan, C. X., Huerta-Espino, J., Lagudah, E. S., Ponce-Molina, L. J. 2017. Identification and mapping of adult plant resistance loci to leaf rust and stripe rust in common wheat cultivar Kundan. Plant Dis. 101:456-463.

Rosewarne, G. M., Herrera-Foessel, S. A., Singh, R. P., Huerta-Espino, J., Lan, C. X., He, Z. H. 2013. Quantitative trait loci of stripe rust resistance in wheat. Theor. Appl. Genet. 126:2427-2449.

Singh, R. P., Mujeeb-Kazi, A., and Huerta-Espino, J. 1998. *Lr46*: a gene conferring slow-rusting to leaf rust in wheat. Phytopathology 88:890–894.

Singh, R. P., Nelson, J. C., and Sorrells, M. E. 2000. Mapping *Yr28* and other genes for resistance to stripe rust in wheat. Crop Sci. 40:1148-1155.

Singh, R. P., Singh, P. K., Rutkoski, J., Hodson, D. P., He, X., Jorgensen, L. N., Hovmoller, M. S., and Huerta-Espino, J. 2016. Disease impact on wheat yield potential and prospects of genetic control. Annu. Rev. Phytopathol. 54:303-322.

Stubbs, R. W. 1985. Stripe rust. Pages 61-101 in: The Cereal Rusts. Vol. II. A. P. Roelfs and W. R. Bushnell, eds. Academic Press, New York.

Vazquez, D. M., Peterson, J. C., Riera-Lizarazu, O., Chen, X., Heesacker, A., Ammar, K., Crossa, J., and Mundt, C. C. 2012. Genetic analysis of adult plant, quantitative resistance to stripe rust in wheat cultivar 'Stephens' in multi-environment trials. Theor. Appl. Genet. 124:1-11.

Voorrips, R. E. 2002. MapChart: Software for the graphical presentation of linkage maps and QTLs. J. Heredity 93:77-78.

Wu, J., Liu, S., Wang, Q., Zeng, Q., Mu, J., Huang, S., Yu, S., Han, D., and Kang, Z. 2018a. Rapid identification of an adult plant stripe rust resistance gene in hexaploid wheat by high-throughput SNP array genotyping of pooled extremes. Theor. Appl. Genet. 131:43-58.

Wu, J., Wang, X., Chen, N., Wang, H., Yu, R., Yu, S., Wang, Q., Huang, S., Singh, R. P., Bhavani, S., Kang, Z., Han, D. J., and Zeng, Q. 2020. Association analysis identifies new loci for resistance to Chinese *Yr26*-virulent races of the stripe rust pathogen in a diverse panel of wheat germplasm. Plant Dis. Doi: 10.1094/PDIS-12-

19-2663-RE.

Wu, J., Zeng, Q., Wang, Q., Liu, S., Yu, S., Mu, J., Huang, S., Sela, H., Distelfeld, A., Huang, L., Han, D., and Kang, Z. 2018b. SNP-based pool genotyping and haplotype analysis accelerate fine-mapping of the wheat genomic region containing stripe rust resistance gene *Yr26*. Theor. Appl. Genet. 131:1481-1496.

Wu, J. H., Wang, Q. L., Chen, X. M., Wang, M. J., Mu, J. M., Lv, X. N., Huang, L. L., Han, D. J., and Kang, Z. S. 2016. Stripe rust resistance in wheat breeding lines developed for central Shaanxi, an overwintering region for *Puccinia striiformis* f. sp. *tritici* in China. Can. J. Plant Pathol. 38:317-324.

Zeng, Q., Han, D., Wang, Q., Yuan, F., Wu, J., Zhang, L., Wang, X., Huang, L., Chen, X., and Kang, Z. 2014. Stripe rust resistance and genes in Chinese wheat cultivars and breeding lines. Euphytica 196:271-284.

Zeng, Q., Wu, J., Liu, S., Chen, X., Yuan, F., Su, P., Wang, Q., Huang, S., Mu, J., Han, D., Kang, Z., Chen, X. M. 2019. Genome-wide mapping for stripe rust resistance loci in common wheat cultivar Qinnong 142. Plant Dis. 103:439-447.

Zhang, P., Hiebert, C. W., McIntosh, R. A., McCallum, B. D., Thomas, J. B., Hoxha, S., Singh, D., and Bansal, U. 2016. The relationship of leaf rust resistance gene *Lr13* and hybrid necrosis gene *Ne2m* on wheat chromosome 2BS. Theor. Appl. Genet. 129:485-493.

Zwart, R. S., Thompson, J. P., Milgate, A. W., Bansal, U. K., Williamson, P. M., Raman, H., and Bariana, H. S. 2010. QTL mapping of multiple foliar disease and root-lesion nematode resistances in wheat. Mol. Breed. 26:107-124.

677 **Figure legends**

678 **Fig. 1.** Frequency distributions of seedling infection type (IT) data for recombinant
679 inbred lines (RILs) derived from AvS × SN33 tested with two *Puccinia striiformis* f.
680 sp. *tritici* isolates (**A**, **B**). **C**, **D**, **E**, and **F**: Distributions of IT data and disease severities
681 (DS) for the RIL population evaluated in 2018 (**A**, **B**) at Yangling (YL) and Jiangyou,
682 and in 2019 (**C**, **D**) at Yangling (YL), Jiangyou (JY), and Tianshui (TS).

683 **Fig. 2.** Genetic map of recombinant inbred lines from the cross AvS × SN33 population.
684 Locations of adult-plant QTL *QYrsn.nwafu-1BL*, *QYrsn.nwafu-2AS.2*, *QYrsn.nwafu-*
685 *3DL*, and *QYrsn.nwafu-6BS* in the linkage maps (**A**, **C**, **E**, and **G**). The regions
686 identified in the BLUP and BLUP analyses were considered the most likely locations
687 (colored red). **B**, **D**, **F**, and **H**: Overlays of previously mapped (black bars) and current
688 (red bars) in integrated genetic maps (Maccaferri et al. 2015; F. Cui, personal
689 communication).

690 **Fig. 3.** Effects of combined quantitative trait loci (QTL) on stripe rust using infection
691 type (**A**) and maximum disease severity (**B**) data for the AvS × SN33 RIL population
692 data from Yangling (YL), Tianshui (TS), and Jiangyou (JY). Y-axes 'QTL combination'

693

694 ## Supplemental Materials

695 **Fig. S1. A** and **B**: Stripe rust responses of SN33 and AvS mid-dough growth stage at
696 Yangling in 2019. **C**: Symptoms of necrosis in homozygous necrotic RIL 59 spike
697 emergence prior to stripe rust development. Necrosis eventually progresses to the flag
698 leaf and leads to lower rust development.

699 **Fig. S2.** Linkage maps and relative locations of seedling resistance QTL *QYrsn.nwafu-*
700 *1DS*, *QYrsn.nwafu-2AS.1*, and *QYrsn.nwafu-3DS* identified in the AvS × SN33 RIL
701 population.

702 **Fig. S3. A**, **B**, and **C**: The performance was described for QTL *QYrsn.nwafu-1BL*,
703 *QYrsn.nwafu-3DL*, and *QYrsn.nwafu-6BS* linked single-nucleotide polymorphism
704 markers in a panel of 420 wheat cultivars and breeding lines, respectively. "+"
705 indicates wheat lines have the same target marker genotypes as in SN33; "-" indicates
706 wheat materials that did not have the target QTL fragment or allele.

707 **Table S1.** Virulence/avirulence formulae of three *Puccinia striiformis* f. sp. *tritici*

isolates used in the study

Table S2. Distribution of single-nucleotide polymorphism (SNP) markers on the 21 wheat chromosomes in the genetic map for the AvS × SN33 RIL population

Table S3. Effects of different QTL combinations in the RILs from the AvS × SN33 population based on infection type (IT) and disease severity (DS) in five field experiments (Yangling, Tianshui, and Jiangyou during the 2017-2019 cropping seasons)

Table S4. The genotyping results of SSR and SNP markers for *QYrsn.nwafu-1BL* (*Yr29*), *QYrsn.nwafu-2AS* (*Yr17*+), and *QYrsn.nwafu-6BS* (*Yr78*) in Shaannong 33, Avocet S, AvSYr17NIL, VPM 1, Madsen, Stephens, and 420 Chinese wheat cultivars and breeding lines

Table S5. Primers of KASP markers for *QYrsn.nawfu-1BL*, *QYrsn.nawfu-3DL*, and *QYrsn.nawfu-6BS*

722 **Table 1.** Correlation coefficients (*r*) of stripe rust infection type (IT) and disease
723 severity (DS) in the AvS × SN33 RIL population across field environments

Environment[a]	*r* value based on DS (IT)[b]			
	2018YL	**2018JY**	**2019JY**	**2019YL**
2018_JY[a]	0.65(0.66)	-	-	-
2019_JY	0.67(0.62)	0.68(0.67)	-	-
2019_YL	0.68(0.64)	0.64(0.63)	0.70(0.71)	-
2019_TS	0.68(0.70)	0.61(0.64)	0.76(0.72)	0.83(0.81)

724 [a] YL, TS, and JY denote Yangling, Tianshui, and Jiangyou, respectively.

725 [b] All *r* values were significant at $P = 0.001$.

726
727

728 **Table 2.** Analysis of variance (ANOVA) for stripe rust infection type (IT) and disease
729 severity (DS) data for the AvS × SN33 RIL population evaluated at Yangling and
730 Jiangyou in 2017 and 2018 and Tianshui in 2018

Source of variation	IT				DS			
	df	**Mean square**	***F* value**	***P*-value**	***df***	**Mean square**	***F* value**	***P*-value**
RILs	148	31.8	30.9	< 0.0001	148	5799.3	30.8	< 0.0001
Replicates	1	3.2	1.3		1	667.6	3.5	
Environments	4	170.7	166.1	< 0.0001	4	26365.1	139.9	< 0.0001
Line × environment	561	3.4	3.3	< 0.0001	560	586.0	3.1	< 0.0001
Error	571	1			571	188.5		
h^2b	0.9				0.9			

731

732 **Table 3.** Summary of stripe rust resistance QTL detected in the AvS × SN33 RIL
733 population in the seedling and adult-pant stages using IciMapping 4.1

Growth stage	QTL	Isolate or enviroment[a]	Marker interval		Genetic position	LOD[b]	PVE[c]	Add[d]
Seedling	*QYrsn.nwafu-1DS*	PST-Lab.1	*AX-110480216*	*AX-111475929*	23	4.0	6.5	-0.6
	QYrsn.nwafu-2AS.1		*AX-108857922*	*AX-111730999*	2	7.1	16.0	-0.9
	QYrsn.nwafu-3DS		*AX-109446046*	*AX-94498685*	2	4.1	9.4	-0.7
	QYrsn.nwafu-1DS	PST-Lab.2	*AX-110480216*	*AX-111475929*	22	12.7	31.5	-1.6
Adult (field)	*QYrsn.nwafu-1BL*	IT-18YL	*AX-108745708*	*AX-110483673*	215	11.0	16.6	-0.8
		DS-18YL	*AX-86184925*	*AX-108745708*	214	8.6	11.7	-7.4
		IT-19YL	*AX-108745708*	*AX-110483673*	215	12.4	18.9	-0.9
		DS-19YL	*AX-108745708*	*AX-110483673*	215	11.4	18.6	-12.9
		IT-18JY	*AX-86184925*	*AX-108745708*	214	8.1	15.6	-0.6
		DS-18JY	*AX-86184925*	*AX-108745708*	213	9.9	15.2	-7.6
		IT-19JY	*AX-111156202*	*AX-86184925*	211	2.9	4.2	-0.4
		DS-19JY	*AX-86184925*	*AX-108745708*	214	4.3	5.0	-5.8
		IT-19TS	*AX-86184925*	*AX-108745708*	214	6.0	8.7	-0.6
		DS-19TS	*AX-108745708*	*AX-110483673*	216	2.8	4.9	-5.6
		IT-BLUP	*AX-111156202*	*AX-86184925*	212	10.4	14.6	-0.6
		DS-BLUP	*AX-111156202*	*AX-86184925*	212	7.0	8.6	-6.2
	QYrsn.nwafu-2AS.2	IT-18YL	*AX-108853005*	*AX-109973606*	3	8.9	13.5	-0.7
		DS-18YL	*AX-108853005*	*AX-109973606*	3	12.7	20.0	-9.7
		IT-19YL	*AX-108857922*	*AX-111730999*	2	7.5	10.4	-0.7
		DS-19YL	*AX-108853005*	*AX-109973606*	3	8.9	13.5	-11.1
		IT-18JY	*AX-108853005*	*AX-109973606*	3	7.6	15.0	-0.6
		DS-18JY	*AX-108857922*	*AX-111730999*	2	13.4	21.5	-9.2
		IT-19JY	*AX-108857922*	*AX-111730999*	2	21.2	36.1	-1.3
		DS-19JY	*AX-108857922*	*AX-111730999*	2	21.3	33.0	-14.9
		IT-19TS	*AX-108857922*	*AX-111730999*	2	10.2	16.6	-0.8
		DS-19TS	*AX-108853005*	*AX-109973606*	3	11.4	22.5	-11.9
		IT-BLUP	*AX-108857922*	*AX-111730999*	2	16.2	24.0	-0.8
		DS-BLUP	*AX-108857922*	*AX-111730999*	2	18.6	26.9	-11.0
	QYrsn.nwafu-3DL	IT-18YL	*AX-111383164*	*AX-111600316*	60	8.0	12.2	-0.7
		DS-18YL	*AX-110950126*	*AX-109582945*	66	9.2	12.2	-7.5
		IT-19YL	*AX-109466386*	*AX-108954437*	54	4.5	5.8	-0.5
		DS-19YL	*AX-109466386*	*AX-108954437*	54	7.3	11.1	-10.0
		IT-18JY	*AX-109582945*	*AX-110284733*	69	4.0	7.3	-0.4
		DS-18JY	*AX-110950126*	*AX-109582945*	66	6.2	8.9	-5.9

	IT-19JY	*AX-110950126*	*AX-109582945*	66	6.5	8.8	-0.6
	DS-19JY	*AX-110950126*	*AX-109582945*	67	7.1	8.8	-7.7
	IT-19TS	*AX-110950126*	*AX-109582945*	66	5.0	7.2	-0.6
	DS-19TS	*AX-110950126*	*AX-109582945*	67	4.5	8.4	-7.3
	IT-BLUP	*AX-110950126*	*AX-109582945*	66	7.4	9.4	-0.5
	DS-BLUP	*AX-110950126*	*AX-109582945*	68	9.0	11.0	-7.0
QYrsn.nwafu-6BS	IT-18YL	*AX-109914013*	*AX-110199811*	61	8.9	13.6	-0.7
	DS-18YL	*AX-108744211*	*AX-110953003*	45	8.4	11.6	-7.3
	IT-19YL	*AX-108908139*	*AX-109914013*	59	12.4	18.5	-0.9
	DS-19YL	*AX-108908139*	*AX-109914013*	58	9.5	15.1	-12.0
	IT-18JY	*AX-109361795*	*AX-108926385*	74	4.5	8.6	-0.4
	DS-18JY	*AX-108744211*	*AX-110953003*	45	6.0	8.5	-5.7
	IT-19JY	*AX-110086144*	*AX-110671936*	52	4.9	6.5	-0.5
	DS-19JY	*AX-110086144*	*AX-110671936*	52	5.9	7.1	-7.0
	IT-19TS	*AX-110602591*	*AX-109325937*	42	7.1	11.3	-0.7
	DS-19TS	*AX-108908139*	*AX-109914013*	57	5.7	10.6	-8.4
	IT-BLUP	*AX-108908139*	*AX-109914013*	58	6.7	8.9	-0.5
	DS-BLUP	*AX-109914013*	*AX-110199811*	61	9.1	11.4	-7.2

734 [a] YL, TS, and JY are abbreviations for Yangling, Tianshui, and Jiangyou, respectively;
735 BLUP = best linear unbiased prediction.

736 [b] LOD, logarithm of odds score.

737 [c] PVE, percentage of the phenotypic variance explained by individual QTL.

738 [d] Add, additive effect of resistance allele. A negative value indicates that the resistance
739 allele is from SN33.

740

Fig. 1

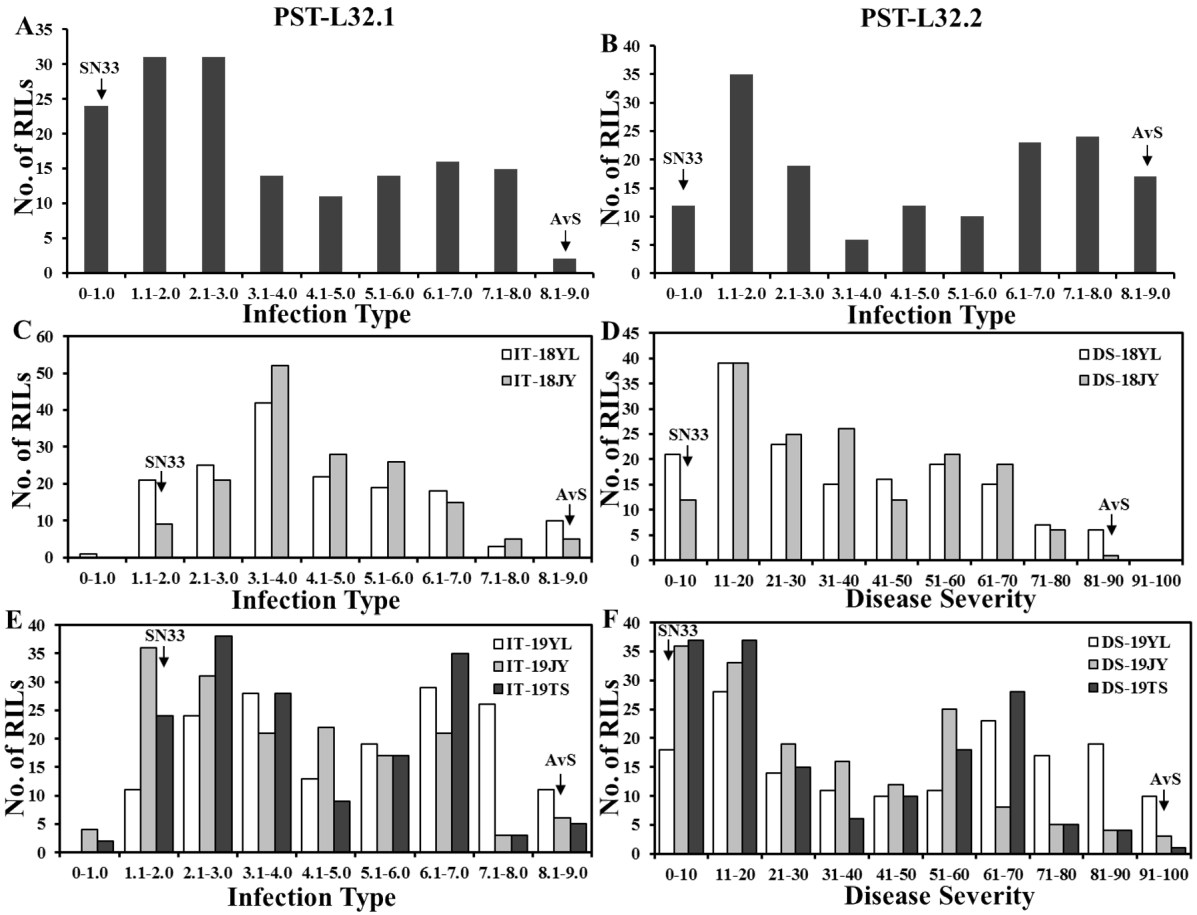
A
PST-L32.1
No. of RILs
SN33
AvS
0-1.0
1.1-2.0
2.1-3.0
3.1-4.0
4.1-5.0
5.1-6.0
6.1-7.0
7.1-8.0
8.1-9.0
Infection Type
B
PST-L32.2
No. of RILs
SN33
AvS
Infection Type
C
No. of RILs
IT-18YL
IT-18JY
SN33
AvS
Infection Type
D
No. of RILs
DS-18YL
DS-18JY
SN33
AvS
0-10
11-20
21-30
31-40
41-50
51-60
61-70
71-80
81-90
91-100
Disease Severity
E
No. of RILs
IT-19YL
IT-19JY
IT-19TS
SN33
AvS
Infection Type
F
No. of RILs
DS-19YL
DS-19JY
DS-19TS
SN33
AvS
Disease Severity

Fig. 2

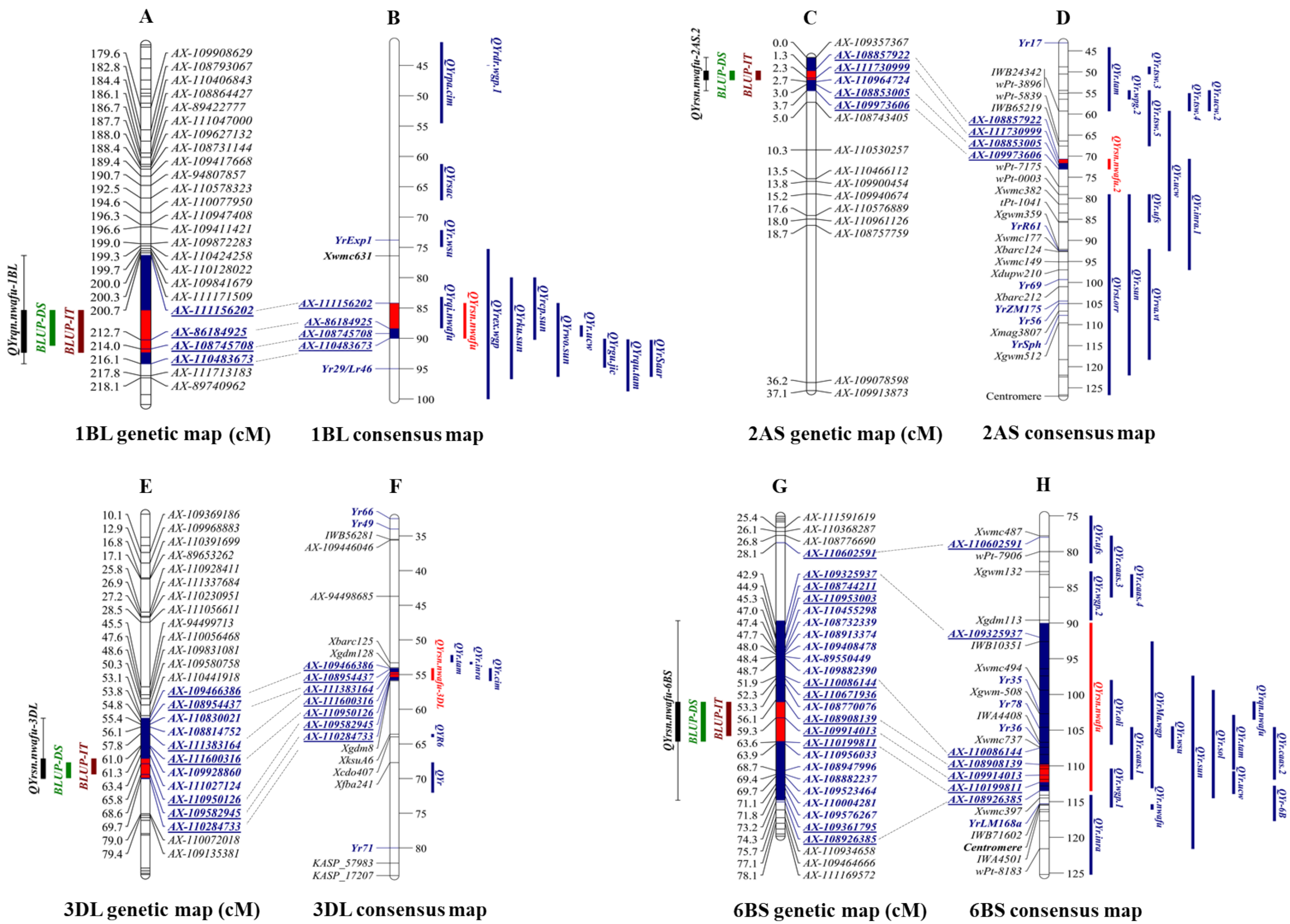
A
B
C
D
E
F
G
H
1BL genetic map (cM)
1BL consensus map
2AS genetic map (cM)
2AS consensus map
3DL genetic map (cM)
3DL consensus map
6BS genetic map (cM)
6BS consensus map
BLUP-DS
BLUP-IT
Centromere

Fig. 3

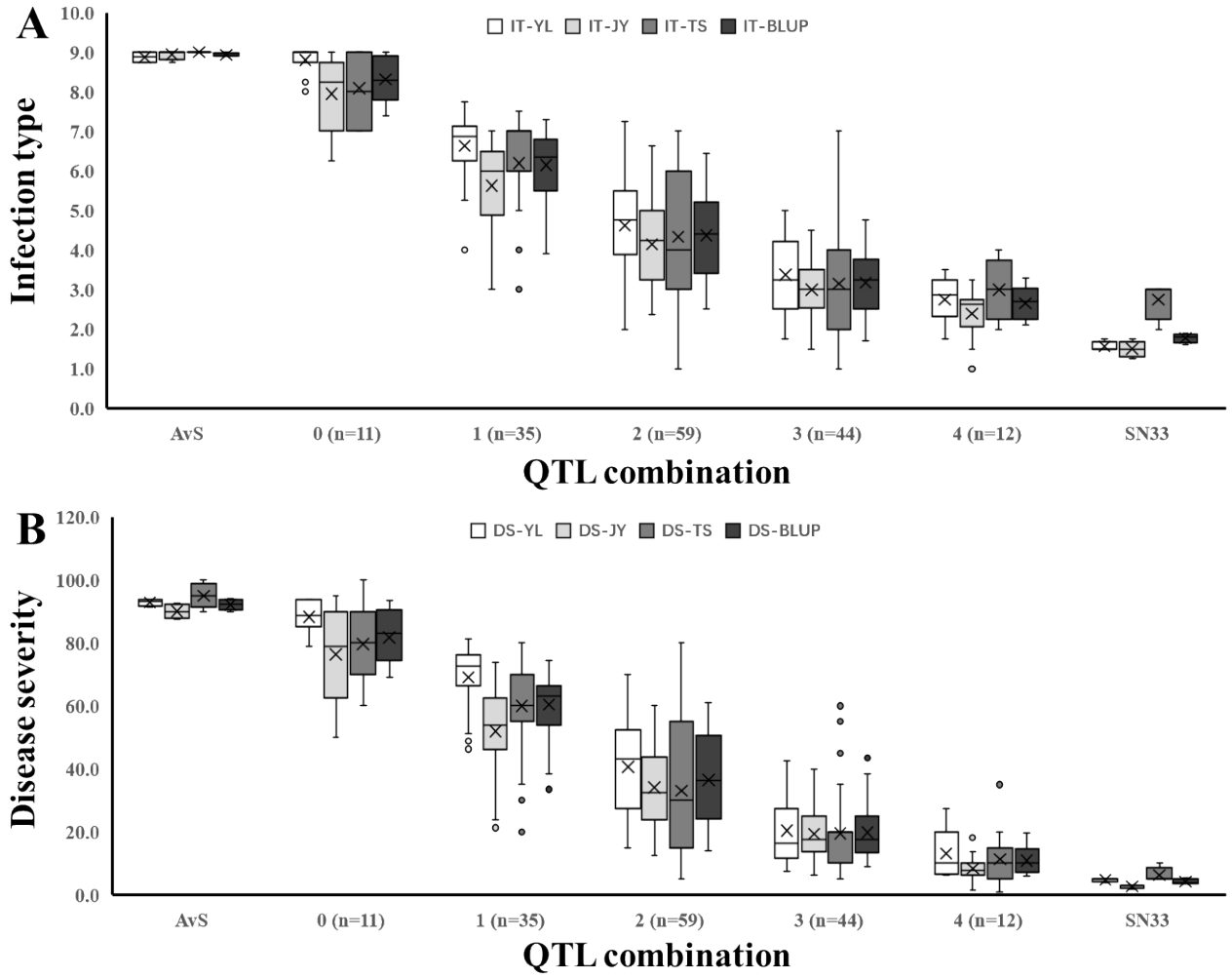
A
IT-YL
IT-JY
IT-TS
IT-BLUP
Infection type
10.0
9.0
8.0
7.0
6.0
5.0
4.0
3.0
2.0
1.0
0.0
AvS
0 (n=11)
1 (n=35)
2 (n=59)
3 (n=44)
4 (n=12)
SN33
QTL combination
B
DS-YL
DS-JY
DS-TS
DS-BLUP
Disease severity
120.0
100.0
80.0
60.0
40.0
20.0
0.0
AvS
0 (n=11)
1 (n=35)
2 (n=59)
3 (n=44)
4 (n=12)
SN33
QTL combination

Fig. S1

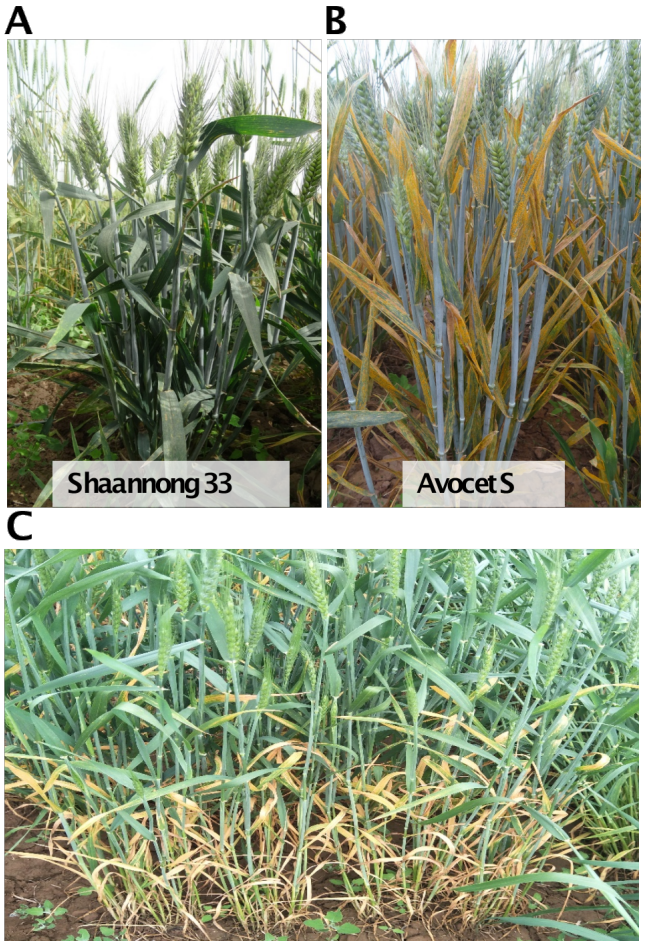

Fig. S2

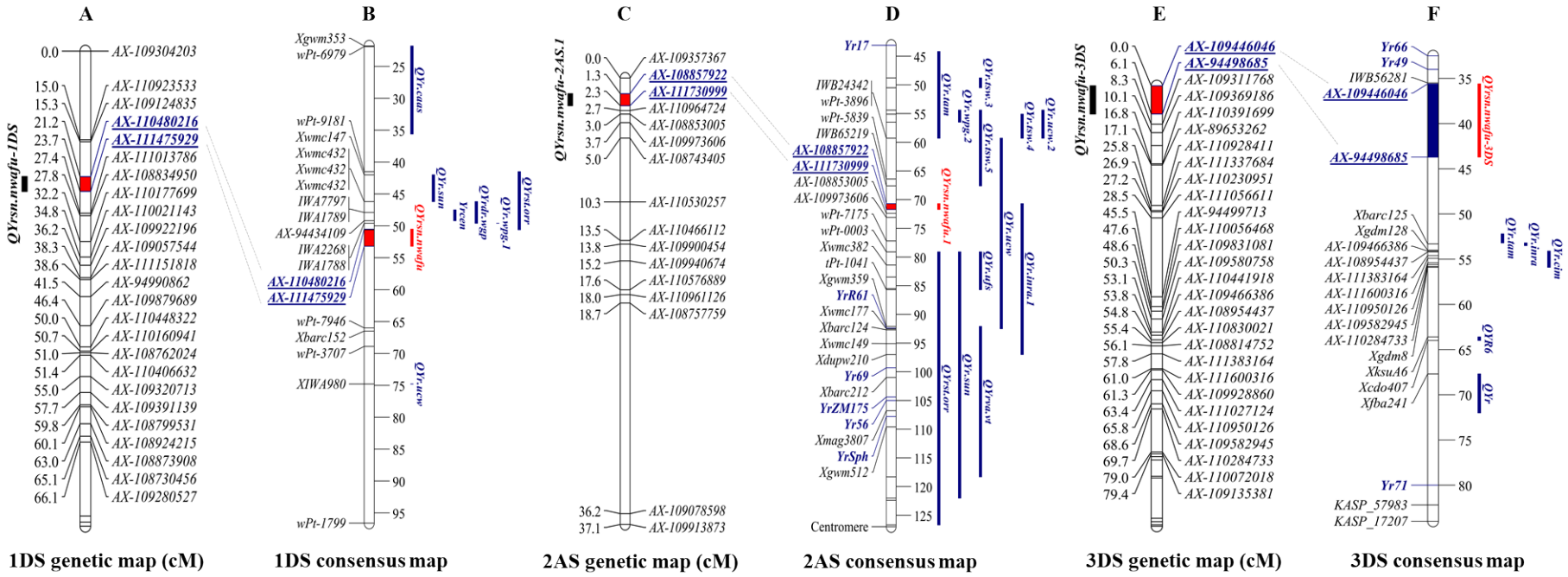
A
B
C
D
E
F
QYrsn.nwafu-1DS
AX-109304203
AX-110923533
AX-109124835
AX-110480216
AX-111475929
AX-111013786
AX-108834950
AX-110177699
AX-110021143
AX-109922196
AX-109057544
AX-111151818
AX-94990862
AX-109879689
AX-110448322
AX-110160941
AX-108762024
AX-110406632
AX-109320713
AX-109391139
AX-108799531
AX-108924215
AX-108873908
AX-108730456
AX-109280527
Xgwm353
wPt-6979
wPt-9181
Xwmc147
Xwmc432
Xwmc432
Xwmc432
IWA7797
IWA1789
AX-94434109
IWA2268
IWA1788
wPt-7946
Xbarc152
wPt-3707
XIWA980
wPt-1799
QYrc.caas
QYrsn
Yrcn
QYrdr.wgp
QYrsn.nwafu
QYrc.wpg-1
QYrslorr
QYrc.acw
QYrsn.nwafu-2AS.1
AX-109357367
AX-108857922
AX-111730999
AX-110964724
AX-108853005
AX-109973606
AX-108743405
AX-110530257
AX-110466112
AX-109900454
AX-109940674
AX-110576889
AX-110961126
AX-108757759
AX-109078598
AX-109913873
Yr17
IWB24342
wPt-3896
wPt-5839
IWB65219
AX-108857922
AX-111730999
AX-108853005
AX-109973606
wPt-7175
wPt-0003
Xwmc382
tPt-1041
Xgwm359
YrR61
Xwmc177
Xbarc124
Xwmc149
Xdupw210
Yr69
Xbarc212
YrZM175
Yr56
Xmag3807
YrSph
Xgwm512
Centromere
QYr.uam
QYrsn.nwafu.1
QYrslorr
QYr.sun
QYr.wgp.2
QYr.sw.3
QYr.sw.5
QYr.acw
QYr.ubj
QYr.sw.4
QYr.acw.2
QYr.inra.1
QYrsw.w
QYrsn.nwafu-3DS
AX-109446046
AX-94498685
AX-109311768
AX-109369186
AX-110391699
AX-89653262
AX-110928411
AX-111337684
AX-110230951
AX-111056611
AX-94499713
AX-110056468
AX-109831081
AX-109580758
AX-110441918
AX-109466386
AX-108954437
AX-110830021
AX-108814752
AX-111383164
AX-111600316
AX-109928860
AX-111027124
AX-110950126
AX-109582945
AX-110284733
AX-110072018
AX-109135381
Yr66
Yr49
IWB56281
Xbarc125
Xgdm128
AX-109466386
AX-108954437
AX-111383164
AX-111600316
AX-110950126
AX-109582945
AX-110284733
Xgdm8
XksuA6
Xcdo407
Xfba241
Yr71
KASP_57983
KASP_17207
QYrsn.nwafu-3DS
QYr.uam
QYr.inra
QYr.cim
QYR6
QYr
1DS genetic map (cM)
1DS consensus map
2AS genetic map (cM)
2AS consensus map
3DS genetic map (cM)
3DS consensus map

Fig. S3